Cell Reports

Report

Loss of *Slc38a4* imprinting is a major cause of mouse placenta hyperplasia in somatic cell nuclear transferred embryos at late gestation

Graphical abstract

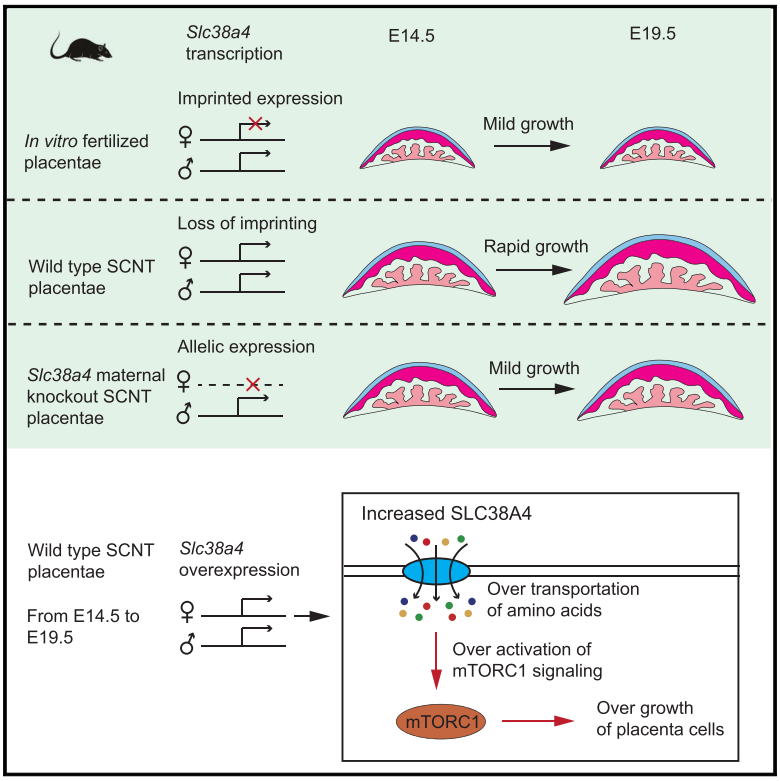

Highlights

- SCNT placenta hyperplasia mostly occurs in middle and late gestation
- Loss of *Slc38a4* imprinting causes SCNT placenta hyperplasia at late gestation
- Loss of *Slc38a4* imprinting over-activates mTORC1 signaling in SCNT placentae
- SLC38A4 likely regulates mTORC1 signaling by modulating amino acids transport

Authors

Zhenfei Xie, Wenhao Zhang, Yi Zhang

Correspondence

yzhang@genetics.med.harvard.edu

In brief

Xie et al. identify loss of H3K27me3-dependent imprinting in *Slc38a4* as a major cause of mouse SCNT placenta hyperplasia at late gestation. The underlying mechanism involves over-activation of mTORC1 signaling in SCNT placentae that likely results from increased amino acid transport by SLC38A4.

Xie et al., 2022, Cell Reports *38*, 110407
February 22, 2022
https://doi.org/10.1016/j.celrep.2022.110407

CellPress

Cell Reports

CellPress
OPEN ACCESS

Report

Loss of *Slc38a4* imprinting is a major cause of mouse placenta hyperplasia in somatic cell nuclear transferred embryos at late gestation

Zhenfei Xie,[1,2,3,6,7] Wenhao Zhang,[1,2,3,7] and Yi Zhang[1,2,3,4,5,8,*]
[1]Howard Hughes Medical Institute, Boston Children's Hospital, Boston, MA 02115, USA
[2]Program in Cellular and Molecular Medicine, Boston Children's Hospital, Boston, MA 02115, USA
[3]Division of Hematology/Oncology, Department of Pediatrics, Boston Children's Hospital, Boston, MA 02115, USA
[4]Department of Genetics, Harvard Medical School, Boston, MA 02115, USA
[5]Harvard Stem Cell Institute, WAB-149G, 200 Longwood Avenue, Boston, MA 02115, USA
[6]The Ragon Institute of Massachusetts General Hospital, Massachusetts Institute of Technology and Harvard University, Cambridge, MA 02139, USA
[7]These authors contributed equally
[8]Lead contact
*Correspondence: yzhang@genetics.med.harvard.edu
https://doi.org/10.1016/j.celrep.2022.110407

SUMMARY

Placenta hyperplasia is commonly observed in cloned animals and is believed to impede the proper development of cloned embryos. However, the mechanism underlying this phenomenon is largely unknown. Here, we show that placenta hyperplasia of cloned mouse embryos occurs in both middle and late gestation. Interestingly, restoring paternal-specific expression of an amino acid transporter *Slc38a4*, which loses maternal H3K27me3-dependent imprinting and becomes biallelically expressed in cloned placentae, rescues the overgrowth of cloned placentae at late gestation. Molecular analyses reveal that loss of *Slc38a4* imprinting leads to over-activation of the mechanistic target of rapamycin complex 1 (mTORC1) signaling pathway in cloned placentae, which is likely due to the increased amino acids transport by SLC38A4. Collectively, our study not only reveals loss of *Slc38a4* imprinting is responsible for overgrowth of cloned placentae at late gestation but also suggests the underlying mechanism involves increased amino acid transport and over-activation of mTORC1.

INTRODUCTION

Somatic cell nuclear transfer (SCNT) technology (also known as cloning) allows reprogramming of differentiated cells into totipotent state that can give rise to cloned animals (Matoba and Zhang, 2018). Despite the success of cloning in many species, cloned animals usually exhibit multiple developmental defects (Smith et al., 2000), of which placenta hyperplasia is frequently observed (Chavatte-Palmer et al., 2012; Gao et al., 2019; Tanaka et al., 2001). Importantly, replacement of the trophoblast lineage of SCNT embryos using fertilization-derived tetraploid embryos could increase the mouse cloning efficiency by 6-fold (Lin et al., 2011), indicating defects in the trophoblast lineage of SCNT embryos significantly contribute to the low cloning efficiency. Therefore, understanding the mechanisms underlying placenta defects may help improve cloning efficiency.

The clue for placenta hyperplasia in cloned animals did not appear until recently, when we discovered that several oocyte-inherited H3K27me3-dependent imprinted genes (e.g., *Sfmbt2*, *Gab1*, *Slc38a4*, *Phf17*, and *Smoc1*) maintain their imprinted states only in extra-embryonic cells, but not in embryonic cells (Chen et al., 2019; Chen and Zhang, 2020; Inoue et al., 2017a, 2018). This leads to loss of imprinting of those genes in SCNT embryos using embryonic cells as donor, resulting in biallelic expression (Matoba et al., 2018). Notably, genetic studies have demonstrated that loss of function of *Sfmbt2*, *Gab1*, or *Slc38a4* results in reduced placenta size and increased embryonic lethality (Inoue et al., 2017b; Matoba et al., 2019; Miri et al., 2013; Sachs et al., 2000). These observations have raised the intriguing possibility that restoring the paternal-specific expression of those genes may rescue placenta overgrowth in cloned animals.

Slc38a4 is a Na^+-coupled neutral amino acids co-transporter that is mainly expressed in placentae (Broer, 2014; Matoba et al., 2019). Loss of *Slc38a4* expression in mouse placentae results in decreased amino acids transportation and reduced placenta growth (Matoba et al., 2019). Although the role of *Slc38a4* in controlling placenta growth is unclear, the change of amino acids concentration in cells could alter mTORC1 signaling pathway, which regulates cell proliferation and growth (Shimobayashi and Hall, 2016).

In this study, we revealed that the placenta hyperplasia of SCNT mice is aggravated in both middle and late gestation. Interestingly, by restoring the paternal-specific expression of *Slc38a4* in SCNT placentae, we demonstrated that loss of

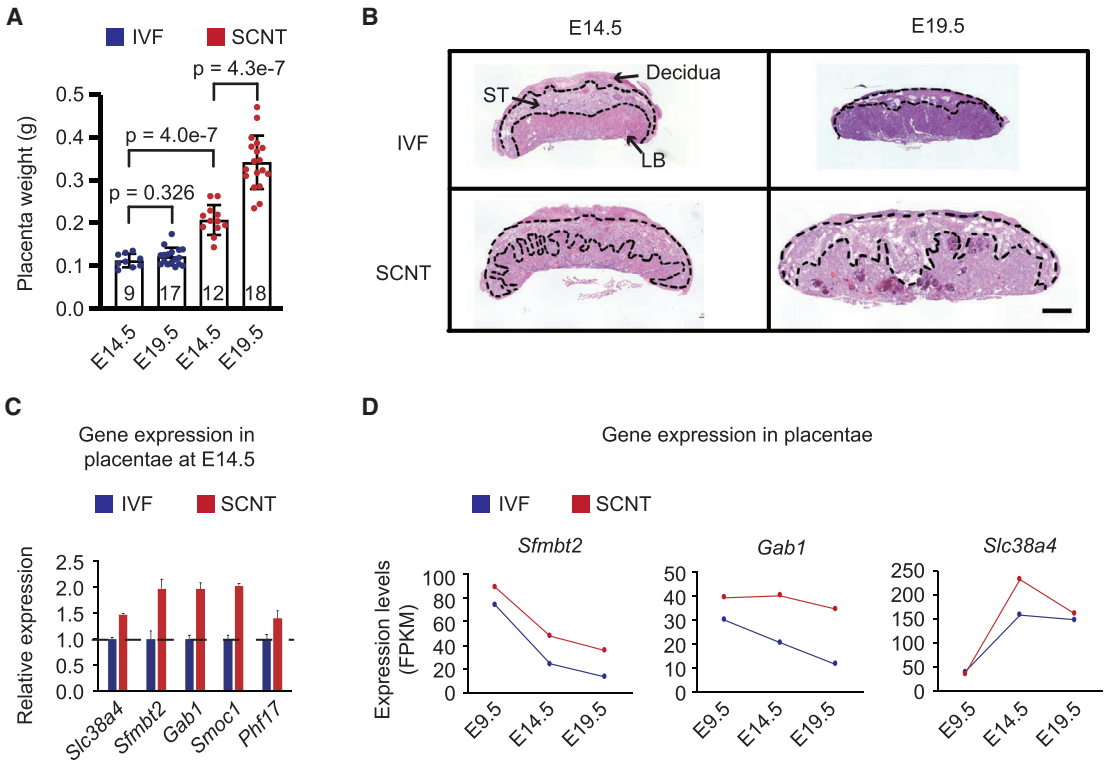

Figure 1. Hyperplasia of mouse SCNT placentae at late gestation correlates with *Slc38a4* overexpression

(A) A bar graph showing placenta weight. Each dot represents placenta of one embryo, and the total number of embryos are indicated in each column. p values are calculated by Student's t test. Error bars represent standard deviation.

(B) Hematoxylin and eosin (H&E) staining of placentae. The dash lines separate decidua, spongiotrophoblast (ST), and labyrinth (LB) in placentae. The scale bar represents 1,000 μm.

(C) A bar graph showing the relative expression levels of H3K27me3-dependent imprinted genes in placentae at E14.5. The average gene expression level in IVF placentae is set as 1. Error bars represent standard deviation.

(D) Plots showing expression levels of *Sfmbt2*, *Gab1*, and *Slc38a4* in placentae. The expression levels are represented by fragments per kilobase per million (FPKM).

See also Figure S1 and Table S1.

Slc38a4 imprinting is a major cause of SCNT placenta hyperplasia, specifically at late gestation. Mechanistically, we showed that loss of *Slc38a4* imprinting in SCNT placentae results in over-transportation of amino acids, which likely over-activates mTORC1 signaling, resulting in overgrowth of SCNT placentae.

RESULTS

Hyperplasia of mouse SCNT placentae occurs in both middle and late gestation

Previous studies have revealed that the placenta growth of normally fertilized mouse embryos mainly takes place in middle gestation (from embryonic day 9.5 [E9.5] to E14.5), when intricate developmental steps occur to form mature placentae, but ceases in late gestation (from E14.5 to E19.5; Jouneau et al., 2006; Woods et al., 2018). To determine when hyperplasia of mouse SCNT placentae takes place, we collected the placentae of *in vitro* fertilized (IVF) and SCNT embryos at E14.5 and E19.5, respectively (Table S1). We found that SCNT placentae (weighted 0.207 ± 0.035 g) at E14.5 are significantly heavier and bigger than IVF placentae (weighted 0.112 ± 0.016 g; p = 4.0×10^{-7}; Figures 1A and 1B). Considering the weight of IVF and SCNT placentae was reported to be similar at E11.5 (Inoue et al., 2020), the initiation of SCNT placenta hyperplasia should occur between E11.5 and E14.5. Next, we analyzed the placenta growth from E14.5 to E19.5. Similar to a previous study (Jouneau et al., 2006), although the IVF placentae at E19.5 (weighted 0.120 ± 0.020 g) did not show much weight difference compared with that at E14.5 (weighted 0.112 ± 0.016 g; p = 0.326; Figures 1A and 1B), the SCNT placentae at E19.5 (weighted 0.337 ± 0.063 g) are significantly heavier and bigger than that at E14.5 (weighted 0.207 ± 0.035 g; p = 4.3×10^{-7}; Figures 1A and 1B). Collectively, our results confirmed that the overgrowth of SCNT placentae not only occurs at middle gestation but also at late gestation, when normal placenta stops growing.

Loss of *Slc38a4* imprinting in SCNT placentae leads to *Slc38a4* overexpression at late gestation

The continued growth of SCNT placentae after E14.5 has attracted our attention. To determine which genes may contribute to this phenomenon, we first investigated the expression dynamics of the H3K27me3-dependent, placenta-specific

imprinted genes (*Sfmbt2*, *Smoc1*, *Gab1*, *Slc38a4*, and *Phf17*), which were proposed to be closely related to SCNT placenta hyperplasia (Matoba et al., 2018). To this end, we profiled transcriptomes of IVF and SCNT placentae at E9.5, E14.5, and E19.5, respectively. Considering the overgrowth of SCNT placentae mainly occurs in the spongiotrophoblast (Tanaka et al., 2001), the transcriptomes were profiled using dissected spongiotrophoblast tissues. After confirming the reproducibility of the transcriptomes (Figure S1A), we analyzed those imprinted genes and found all of them showed 1.5- to 2.0-fold increase of expression in SCNT placentae compared with that in IVF placentae at E14.5 (Figure 1C), consistent with our previous report that these imprinted genes exhibit biallelic expression in SCNT embryos (Matoba et al., 2018).

Since three of these genes, *Sfmbt2*, *Gab1*, and *Slc38a4*, have been previously reported to be important for placenta growth (Inoue et al., 2017b; Matoba et al., 2019; Miri et al., 2013; Sachs et al., 2000), we compared their expression dynamics in IVF and SCNT placentae from E9.5 to E19.5. We found that the expression of *Sfmbt2* and *Gab1* has reached the highest level at E9.5 and then keeps decreasing in middle and late gestation of IVF and SCNT placentae. In contrast, the expression of *Slc38a4* shows dramatic increase during middle gestation and is maintained at a high level at late gestation (Figure 1D). Notably, although analysis of a public dataset indicates *Slc38a4* has already switched from paternal to biallelic expression in SCNT placentae before E10.5 (Wang et al., 2020; Figure S1B), overexpression of *Slc38a4* in SCNT placentae mainly appears later at around E14.5 (Figure 1D), indicating the developmental defects caused by loss of *Slc38a4* imprinting likely happen at late gestation. This makes *Slc38a4* a good candidate for explaining the continued growth of SCNT placentae from E14.5 to E19.5.

Maternal knockout of *Slc38a4* rescues overgrowth of SCNT placentae specifically at late gestation

To restore paternal-specific expression of *Slc38a4* in SCNT embryos, one strategy is to use donor cells with the maternal allele of *Slc38a4* knocked out. To this end, we generated *Slc38a4* mutant mice using the CRISPR-Cas9 system to delete exon 3 (91 bp) of *Slc38a4*, resulting in a frameshift mutation (Figures 2A and S2A). Since most *Slc38a4* homozygous or paternal knockout mice cannot survive more than 3 weeks after birth (Matoba et al., 2019), we generated mosaic knockout female mice by injecting *Cas9* mRNA and *Slc38a4* guide RNAs into one blastomere of the two-cell embryos (Figure 2A). After confirming successful deletion of exon 3 of *Slc38a4* in the female mice (Figure S2A), we mated them with wild-type (WT) male mice. Then, cumulus cells from female offspring with maternal knockout (MKO) of *Slc38a4* were used for SCNT (MKO SCNT) (Figure 2A). Cumulus cells from WT female mice were used as control (WT SCNT). The SLC38A4 protein in MKO SCNT placentae has been restored to a level comparable with that in IVF placentae (Figure S2B), confirming the successful maternal knockout of *Slc38a4*.

Although no significant differences in implantation rate and live embryo and pup rate were observed between WT SCNT and MKO SCNT at E14.5 or E19.5 (Figure 2B), we found WT SCNT placentae are significantly heavier and bigger than MKO SCNT placentae at E19.5 (average weight difference = 0.089 g; $p = 1.5 \times 10^{-4}$; Figures 2C and 2D; Table S1). Importantly, WT SCNT placentae exhibited a large weight increase from E14.5 to E19.5 (increased 0.130 g in average), while IVF and MKO SCNT placentae only showed a mild weight increase during the same period (increased 0.008 g and 0.046 g in average, respectively; Figures 2D and 2E; Table S1). Furthermore, consistent with the previous study showing spongiotrophoblast is the major tissue that expands in SCNT placentae (Tanaka et al., 2001), we found the ratio of spongiotrophoblast versus labyrinth is significantly increased in WT SCNT placentae compared with that in IVF placentae from E14.5 to E19.5 (Figures 1B and 2F). However, such abnormal increase is largely rescued in MKO SCNT placentae (Figures 2C and 2F). In contrast to placentae, the weight of IVF, WT SCNT, and MKO SCNT embryos exhibited no significant difference (Figures S2C and S2D; Table S1). Taken together, the above results indicate that *Slc38a4* overexpression caused by loss of H3K27me3 imprinting in SCNT placentae is a major cause of the continued placenta overgrowth with spongiotrophoblast expansion at late gestation.

Loss of *Slc38a4* imprinting leads to over-activation of mTORC1 signaling in SCNT placentae at late gestation

To gain insights into the mechanism by which loss of *Slc38a4* imprinting leads to SCNT placenta hyperplasia, we profiled the transcriptomes of MKO SCNT placentae using dissected spongiotrophoblast tissues at E14.5 and E19.5. After verifying the reproducibility of the transcriptomes (Figure S3A), we confirmed that the expression of *Slc38a4* in MKO SCNT placentae has been restored to a level similar to that in IVF placentae at E14.5 (Figure S3B), which is consistent with the detected changes of SLC38A4 protein levels (Figure S2B). In contrast, the other H3K27me3 imprinted genes still show overexpression in *Slc38a4* MKO SCNT placentae (Figure S3B).

To determine the effect of transcriptomic changes in SCNT placentae caused by loss of *Slc38a4* imprinting, we performed comparative analysis of transcriptomes between WT SCNT and MKO SCNT placentae at both E14.5 and E19.5. While only 164 upregulated and 162 downregulated genes in MKO SCNT placentae compared with WT SCNT placentae were identified at E14.5, the same analysis revealed 1,757 upregulated and 476 downregulated genes in MKO SCNT placentae compared with WT SCNT placentae at E19.5 (Figure 3A; Table S2), indicating the effects of *Slc38a4* overexpression in SCNT placentae become severe during late gestation. This is consistent with our observation that restoring paternal-specific expression of *Slc38a4* rescued SCNT placenta overgrowth, mainly at late gestation (Figures 2C–2F). Thus, we mainly focused on the placenta transcriptomes at E19.5. An initial analysis revealed a significant number of genes were dysregulated in WT SCNT placentae compared with IVF placentae, which were relieved in MKO SCNT placentae (Figure 3B; Table S2). To better select out the dysregulated genes related to *Slc38a4* overexpression in SCNT placentae, we set a cutoff of 1.5-fold change in expression levels and identified 330 and 584 genes, which were respectively up- and downregulated in WT SCNT placentae compared with IVF placentae and were rescued in MKO SCNT placentae (Figure 3C; Table S2). Ingenuity pathway analysis (IPA) of these

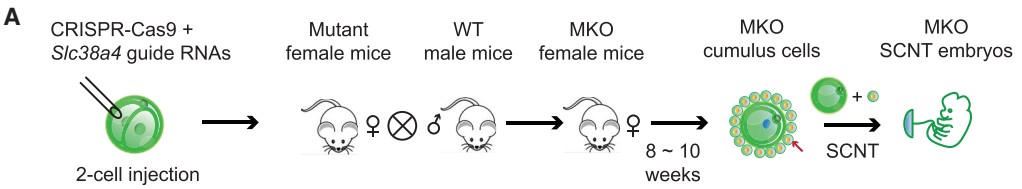

B

	2-cell embryos transferred	Recipient mothers	Implantation rate	Live embryo /pup rate
WT SCNT (E14.5)	304	13	171/304 (56.3%)	13/304 (4.3%)
MKO SCNT (E14.5)	178	10	98/178 (55.1%)	7/178 (3.9%)
WT SCNT (E19.5)	514	29	288/514 (56.0%)	18/514 (3.5%)
MKO SCNT (E19.5)	352	18	176/352 (50.0%)	12/352 (3.4%)

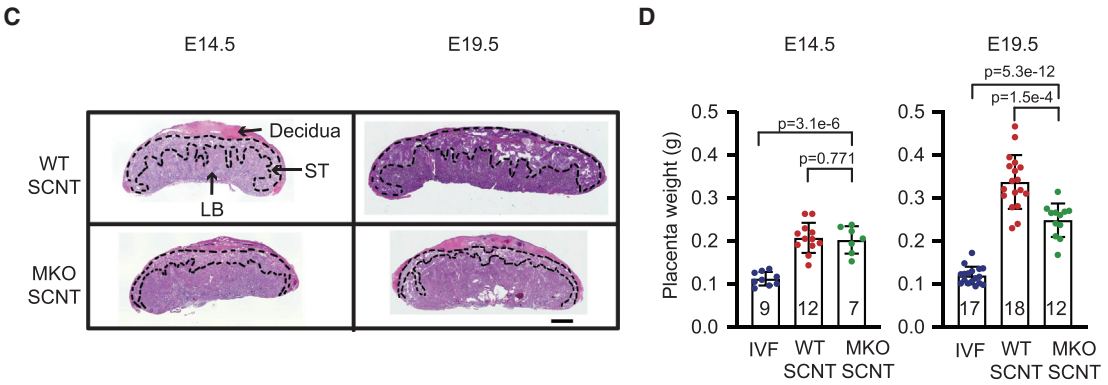

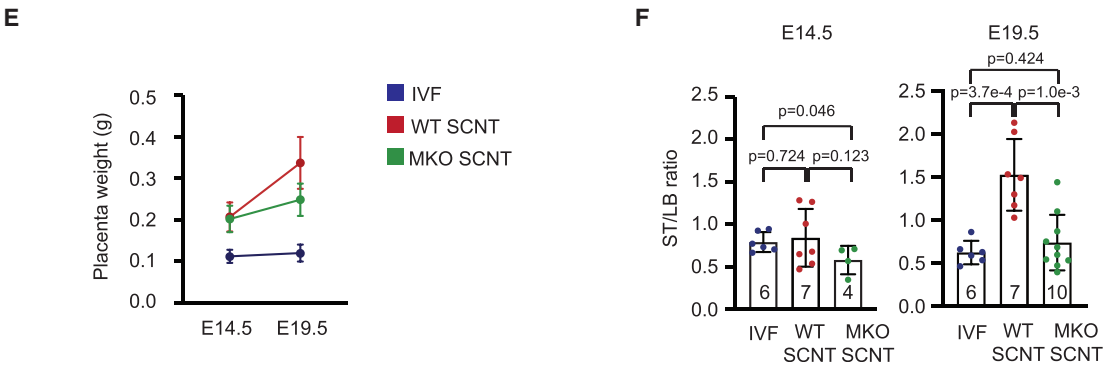

Figure 2. Restoring paternal-specific expression of *Slc38a4* rescues overgrowth of SCNT placentae at late gestation

(A) A schematic presentation of the strategy for generating *Slc38a4* MKO female mice for SCNT.

(B) A table summarizing SCNT experiments in this study.

(C) H&E staining of placentae. The dash lines separate decidua, ST, and LB in placentae. The scale bar represents 1,000 μm.

(D) Bar graph showing placenta weight. Each dot represents placenta of one embryo, and the total number of embryos is indicated in each column. p values are calculated by Student's t test. Error bars represent standard deviation.

(E) Plots showing average placenta weight. Error bars represent standard deviation.

(F) Bar graph showing the area ratio of ST versus LB in placentae. Each dot represents placenta of one embryo, and the total number of embryos is indicated in each column. p values are calculated by Student's t test. Error bars represent standard deviation.

See also Figure S2 and Table S1.

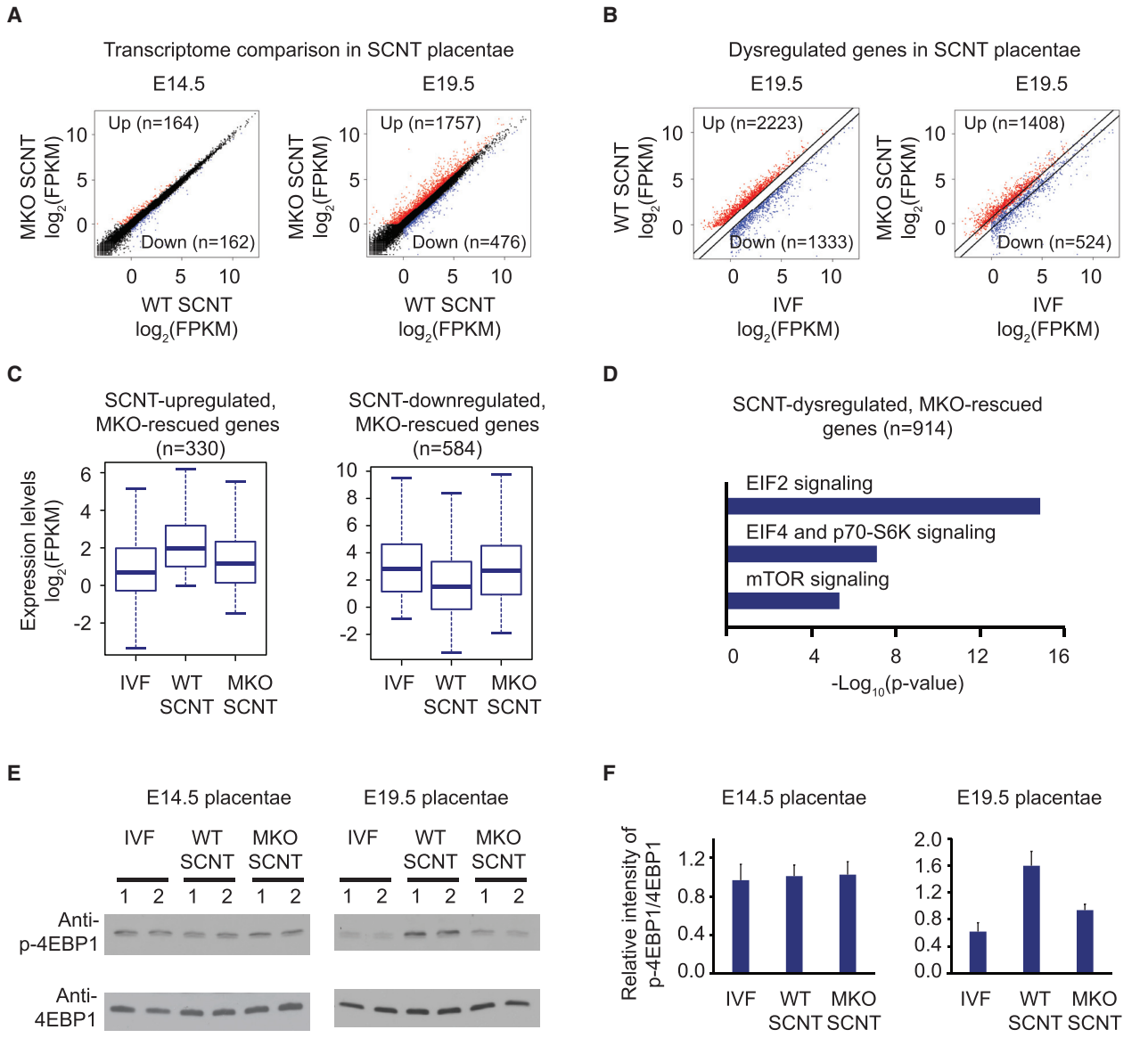

Figure 3. Loss of *Slc38a4* imprinting leads to mTORC1 over-activation in SCNT placentae at late gestation

(A) Scatterplots comparing gene expression between WT SCNT and MKO SCNT placentae. Genes up- (red) and downregulated (blue) in MKO SCNT placentae were marked.

(B) Scatterplots showing expression levels of all genes up- (red) and downregulated (blue) in WT SCNT placentae compared with IVF placentae.

(C) Boxplots showing genes up- and downregulated in WT SCNT placentae compared with IVF placentae and rescued in MKO SCNT placentae.

(D) Ingenuity pathway analysis (IPA) showing enriched pathways for the genes rescued in MKO SCNT placentae related to (C). p values for each category are presented.

(E) Protein levels of p-4EBP1and 4EBP1 in placentae at E14.5 and E19.5, with biological replicates presented.

(F) Statistical calculation of p-4EPB1/4EBP1 ratio in placentae related to (E) and Figure S3D. Error bars represent standard deviation.

See also Figure S3 and Table S2.

rescued genes revealed the top three ranked pathways were "EIF2 signaling," "EIF4 and p70-S6K signaling," and "mTOR signaling" (Figure 3D). Since EIF4 and p70-S6K are downstream effectors of mTORC1 signaling pathway (Kim and Guan, 2019; Laplante and Sabatini, 2012), while EIF2 is closely related to mTORC1 signaling pathway (Wengrod and Gardner, 2015), mTORC1 signaling pathway became our focus. Given that mTORC1 plays an important role in regulating cell growth and proliferation (Laplante and Sabatini, 2012), loss of *Slc38a4* imprinting may disrupt mTORC1 signaling, resulting in SCNT placenta overgrowth. Consistently, Gene Ontology analysis of the rescued genes showed significant enrichment in terms of "translation," "ribosomal small subunit assembly," and "regulation of cell growth" (Figure S3C).

Since mTORC1 signaling is mainly regulated at protein level, we examined the level of phosphorylated 4EBP1 (p-4EBP1), a typical downstream target of mTORC1 (Kim and Guan, 2019; Shimobayashi and Hall, 2016), as an indicator of mTORC1 activity. The total 4EBP1 level served as a control. We found, although the p-4EBP1 level is similar in IVF, WT SCNT, and MKO SCNT placentae at E14.5, it is clearly higher in WT SCNT placentae compared with that in IVF and MKO SCNT placentae at E19.5 (Figures 3E and S3D). A statistical analysis calculating the relative intensity of p-4EBP1/4EBP1 further confirmed this observation (Figure 3F). Collectively, the above results suggest that loss of *Slc38a4* imprinting in SCNT placentae over-activates mTORC1 signaling at late gestation.

Loss of *Slc38a4* imprinting in SCNT placentae causes over-transportation of amino acids

Next, we explored the link between *Slc38a4* overexpression (due to loss of imprinting) and mTORC1 over-activation in SCNT placentae. SLC38A4 functions to import amino acids into cells and is mainly expressed in placenta (Broer, 2014; Matoba et al., 2019). Interestingly, amino acids are well-known modulators of the mTORC1 signaling pathway (Kim and Guan, 2019; Shimobayashi and Hall, 2016; see details in Figure S4A). Thus, amino acids likely serve as linkers between dysregulated *Slc38a4* and mTORC1 signaling in SCNT placentae. Nevertheless, it remains to be shown whether loss of *Slc38a4* imprinting can indeed disrupt amino acid transportation in SCNT placentae and, if so, which amino acids are affected. Considering the fetal placentae can be easily contaminated by mother's blood and the nutrients absorbed by the placenta cells can be transferred directly into fetal blood (Aplin et al., 2020; Matoba et al., 2019), we profiled metabolomes of fetal blood serum at E19.5 to indicate the biomolecules transported by placentae (Table S3). After confirming the reproducibility of the metabolomes from independent samples (Figure S4B), we performed principal-component analysis (PCA), which revealed three groups separating IVF, WT SCNT, and MKO SCNT fetal blood serum (Figure S4C), indicating metabolome differences exist among the three groups (Figure S4B). Using $p < 0.05$ as a cutoff, we identified 18 upregulated and 8 downregulated biomolecules in blood serum of WT SCNT fetuses, compared with that of IVF fetuses (Figure 4A; Table S3). Interestingly, the percentage of upregulated amino acids in total detected amino acids (37.5%) is clearly higher than that of upregulated biomolecules in total detected biomolecules (7.8%), indicating amino acid is a major type of dysregulated biomolecules in SCNT (Figure 4A).

The amino acids significantly increased in blood serum of WT SCNT fetuses include cysteine, valine, leucine and isoleucine, arginine, phenylalanine, and histidine (Figure 4B). Interestingly, these amino acids all decreased in the blood serum of MKO SCNT fetuses to a level comparable with that in IVF fetuses (Figure 4B), indicating SLC38A4-transported amino acids were decreased in MKO SCNT placentae compared with that in WT SCNT placentae. These results support our notion that loss of *Slc38a4* imprinting in WT SCNT placentae results in over-transportation of amino acids into placenta cells, which likely over-activates mTORC1 signaling pathway, leading to the continued overgrowth of SCNT placentae at late gestation.

DISCUSSION

During the preparation of this manuscript, two studies reported loss of *Sfmbt2* imprinting in SCNT placentae (which also leads to overexpression of a microRNA cluster in its intron 10) contributes to SCNT placenta overgrowth (Inoue et al., 2020; Wang et al., 2020). Interestingly, our study showed restoring paternal-specific expression of *Slc38a4* in SCNT placentae barely affects placenta overgrowth before E14.5 but largely prevents placenta overgrowth from E14.5 to E19.5 (Figures 2C–2E), though loss of *Sfmbt2* imprinting is not corrected (Figure S3B). Collectively, these studies together suggest that loss of H3K27me3 imprinting on *Sfmbt2* and *Slc38a4* is majorly responsible for SCNT placenta overgrowth at middle and late gestation, respectively (Figure 4C).

Notably, the study by Inoue et al. (2020) reported that WT SCNT placentae (weighted 0.328 ± 0.020 g) and *Slc38a4* MKO SCNT placentae (weighted 0.280 ± 0.010 g) are both significantly heavier than IVF placentae (weighted 0.107 ± 0.004 g), which led them to conclude that biallelic expression of *Slc38a4* may not be a primary cause of SCNT placenta hyperplasia. However, only six WT SCNT placentae and three *Slc38a4* MKO SCNT placentae at E19.5 were analyzed in their study (Inoue et al., 2020). Although a similar trend of reduced growth in MKO SCNT placentae is observed, considering the variation of individual samples in SCNT experiments, the limited number of samples probably has made the differences statistically insignificant.

Finally, our study indicates lacking a full set of gemmate-derived genomic imprints in SCNT donor cells is likely a major reason for the abnormal development of SCNT embryos, especially at post-implantation stages. Similarly, oocyte-inherited imprints in monkey are preferentially maintained in placenta cells, but not in somatic cells, resulting in severe imprinting defects in monkey SCNT placentae (Chu et al., 2021), which may contribute to the extremely low efficiency and quality of primate cloning (Liu et al., 2018). In the future, more studies on the tissue-specific imprinting will significantly facilitate our understanding of the developmental defects in cloned animals.

Limitation of the study

In this study, we have showed SCNT placenta hyperplasia at late gestation is majorly caused by loss of *Slc38a4* imprinting, which likely over-activates mTORC1 signaling through over-transportation of amino acids. However, we cannot rule out whether other unknown mechanisms exist. We also did not explore the detailed mechanisms of how over-transported amino acids by SLC38A4 may trigger mTORC1 hyperactivity in SCNT placentae. Future studies focusing on the regulation of mTORC1 signaling pathway in SCNT placentae may help clarify these questions.

STAR★METHODS

Detailed methods are provided in the online version of this paper and include the following:

- KEY RESOURCES TABLE
- RESOURCE AVAILABILITY

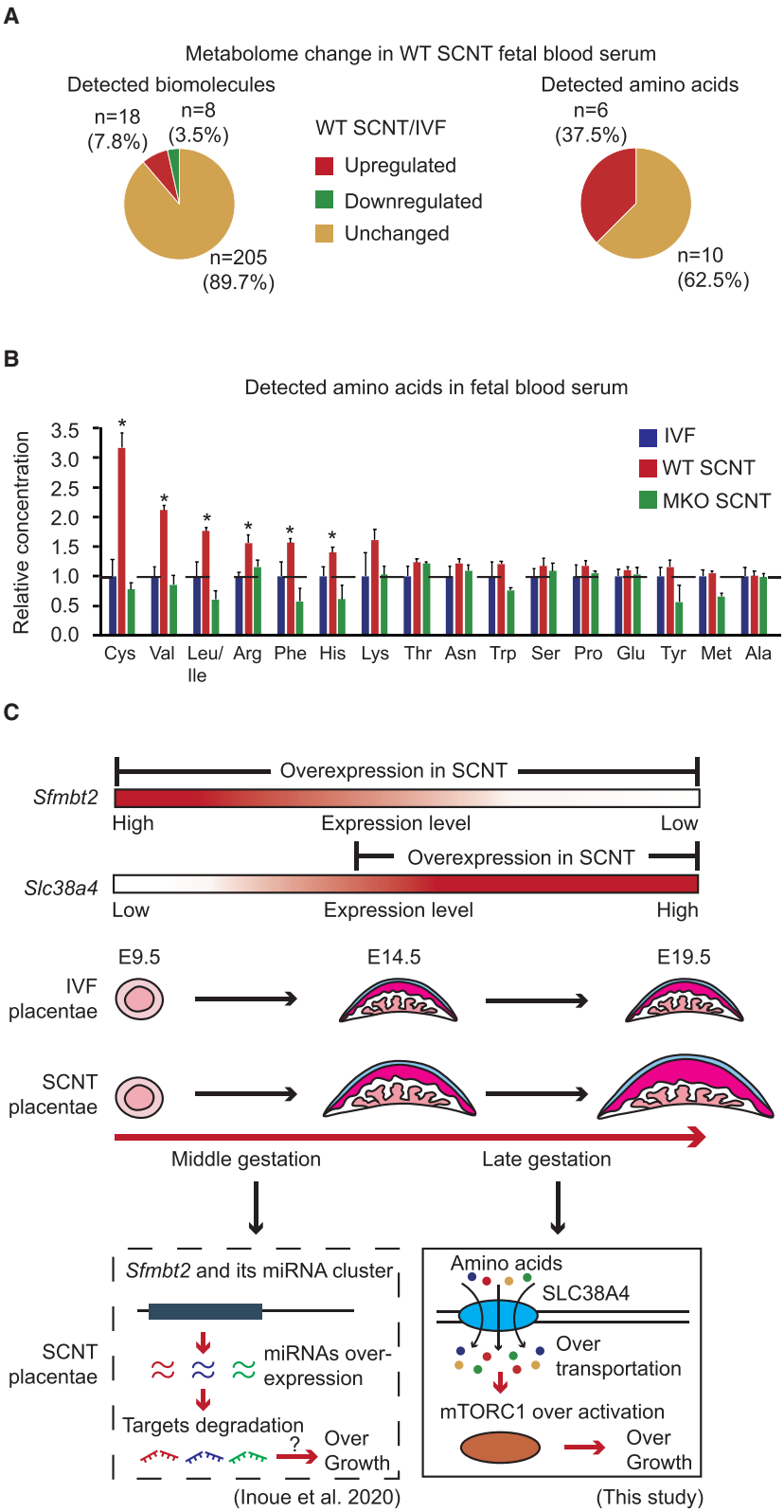

Figure 4. Loss of *Slc38a4* imprinting in SCNT placentae causes over-transportation of amino acids

(A) Pie charts showing overall changes of biomolecules and amino acids between IVF and SCNT fetal blood serum.

(B) A bar graph showing relative concentration of amino acids normalized to that in IVF fetal blood serum. Asterisks indicate significantly upregulated amino acids in blood serum of WT SCNT fetuses compared with that of IVF fetuses ($p < 0.05$, calculated by Student's t test). Error bars represent standard deviation.

(C) A schematic model explaining the major causes of mouse SCNT placenta hyperplasia. Briefly, loss of *Sfmbt2* imprinting leads to overexpression of the microRNA cluster in its intron 10, which majorly contributes to placenta overgrowth at middle gestation. Loss of *Slc38a4* imprinting leads to over-transportation of amino acids and over-activation of mTORC1, which majorly contributes to placenta overgrowth at late gestation. Consistently, the expression levels of *Sfmbt2* and *Slc38a4* in placentae peak in middle gestation and late gestation, respectively.

See also Figure S4 and Table S3.

SUPPLEMENTAL INFORMATION

Supplemental information can be found online at https://doi.org/10.1016/j.celrep.2022.110407.

ACKNOWLEDGMENTS

We thank members of the Zhang lab, Drs. Zhiyuan Chen, Chunxia Zhang, and Yuangao Wang, for helpful discussion and comments on the manuscript. This project was supported by the NIH (R01HD092465) and HHMI. Y.Z. is an Investigator of the Howard Hughes Medical Institute.

AUTHOR CONTRIBUTIONS

Y.Z. conceived and supervised the project. Z.X. and W.Z. generated *Slc38a4* maternal knockout mice. Z.X. performed the SCNT experiments. Z.X. and W.Z. analyzed the placenta phenotype. W.Z. performed western blot, RNA sequencing, and the data analysis. Z.X. and W.Z. analyzed the metabolomes of blood serum. Y.Z. and W.Z. wrote the manuscript with inputs from Z.X.

DECLARATION OF INTERESTS

The authors declare no competing interests.

Received: June 10, 2021
Revised: November 2, 2021
Accepted: January 26, 2022
Published: February 22, 2022

SUPPORTING CITATIONS

The following reference appears in the Supplemental information: Chantranupong et al., 2014; Kim et al., 2015; Parmigiani et al., 2014; Petit et al., 2013; Rebsamen et al., 2015; Sancak et al., 2008; Thomas et al., 2014; Tsun et al., 2013; Wolfson et al., 2016.

REFERENCES

Aplin, J.D., Myers, J.E., Timms, K., and Westwood, M. (2020). Tracking placental development in health and disease. Nat. Rev. Endocrinol. *16*, 479–494.

Broer, S. (2014). The SLC38 family of sodium-amino acid co-transporters. Pflugers Arch. *466*, 155–172.

Chantranupong, L., Wolfson, R.L., Orozco, J.M., Saxton, R.A., Bar-Peled, L., Spooner, E., Isasa, M., Gygi, S.P., and Sabatini, D.M. (2014). The Sestrins interact with GATOR2 to negatively regulate the amino-acid-sensing pathway upstream of mTORC1. Cell Report *9*, 1–8.

Chavatte-Palmer, P., Camous, S., Jammes, H., Le Cleac'h, N., Guillomot, M., and Lee, R.S. (2012). Review: placental perturbations induce the developmental abnormalities often observed in bovine somatic cell nuclear transfer. Placenta *33*, S99–S104.

Chen, Z., Yin, Q., Inoue, A., Zhang, C., and Zhang, Y. (2019). Allelic H3K27me3 to allelic DNA methylation switch maintains noncanonical imprinting in extraembryonic cells. Sci. Adv. *5*, eaay7246.

Chen, Z., and Zhang, Y. (2020). Maternal H3K27me3-dependent autosomal and X chromosome imprinting. Nat. Rev. Genet. *21*, 555–571.

Chu, C., Zhang, W., Kang, Y., Si, C., Ji, W., Niu, Y., and Zhang, Y. (2021). Analysis of developmental imprinting dynamics in primates using SNP-free methods to identify imprinting defects in cloned placenta. Dev. Cell *56*, 2826–2840.e7.

Danecek, P., Auton, A., Abecasis, G., Albers, C.A., Banks, E., DePristo, M.A., Handsaker, R.E., Lunter, G., Marth, G.T., Sherry, S.T., et al. (2011). The variant call format and VCFtools. Bioinformatics *27*, 2156–2158.

Gao, G., Wang, S., Zhang, J., Su, G., Zheng, Z., Bai, C., Yang, L., Wei, Z., Wang, X., Liu, X., et al. (2019). Transcriptome-wide analysis of the SCNT bovine abnormal placenta during mid- to late gestation. Sci. Rep. *9*, 20035.

Huang da, W., Sherman, B.T., and Lempicki, R.A. (2009). Systematic and integrative analysis of large gene lists using DAVID bioinformatics resources. Nat. Protoc. *4*, 44–57.

Inoue, A., Chen, Z., Yin, Q., and Zhang, Y. (2018). Maternal Eed knockout causes loss of H3K27me3 imprinting and random X inactivation in the extraembryonic cells. Genes Dev. *32*, 1525–1536.

Inoue, A., Jiang, L., Lu, F., Suzuki, T., and Zhang, Y. (2017a). Maternal H3K27me3 controls DNA methylation-independent imprinting. Nature *547*, 419–424.

Inoue, K., Hirose, M., Inoue, H., Hatanaka, Y., Honda, A., Hasegawa, A., Mochida, K., and Ogura, A. (2017b). The rodent-specific MicroRNA cluster within the Sfmbt2 gene is imprinted and essential for placental development. Cell Rep. *19*, 949–956.

Inoue, K., Ogonuki, N., Kamimura, S., Inoue, H., Matoba, S., Hirose, M., Honda, A., Miura, K., Hada, M., Hasegawa, A., et al. (2020). Loss of H3K27me3 imprinting in the Sfmbt2 miRNA cluster causes enlargement of cloned mouse placentas. Nat. Commun. *11*, 2150.

Jouneau, A., Zhou, Q., Camus, A., Brochard, V., Maulny, L., Collignon, J., and Renard, J.P. (2006). Developmental abnormalities of NT mouse embryos appear early after implantation. Development *133*, 1597–1607.

Kim, D., Pertea, G., Trapnell, C., Pimentel, H., Kelley, R., and Salzberg, S.L. (2013). TopHat2: accurate alignment of transcriptomes in the presence of insertions, deletions and gene fusions. Genome Biol. *14*, R36.

Kim, J., and Guan, K.L. (2019). mTOR as a central hub of nutrient signalling and cell growth. Nat. Cell Biol. *21*, 63–71.

Kim, J.S., Ro, S.H., Kim, M., Park, H.W., Semple, I.A., Park, H., Cho, U.S., Wang, W., Guan, K.L., Karin, M., et al. (2015). Sestrin2 inhibits mTORC1 through modulation of GATOR complexes. Sci Rep *5*, 9502.

Kishigami, S., Wakayama, S., Thuan, N.V., Ohta, H., Mizutani, E., Hikichi, T., Bui, H.T., Balbach, S., Ogura, A., Boiani, M., et al. (2006). Production of cloned mice by somatic cell nuclear transfer. Nat. Protoc. *1*, 125–138.

Laplante, M., and Sabatini, D.M. (2012). mTOR signaling in growth control and disease. Cell *149*, 274–293.

Lin, J., Shi, L., Zhang, M., Yang, H., Qin, Y., Zhang, J., Gong, D., Zhang, X., Li, D., and Li, J. (2011). Defects in trophoblast cell lineage account for the impaired in vivo development of cloned embryos generated by somatic nuclear transfer. Cell Stem Cell *8*, 371–375.

Liu, Z., Cai, Y., Wang, Y., Nie, Y., Zhang, C., Xu, Y., Zhang, X., Lu, Y., Wang, Z., Poo, M., et al. (2018). Cloning of macaque monkeys by somatic cell nuclear transfer. Cell *172*, 881–887.e7.

Matoba, S., Nakamuta, S., Miura, K., Hirose, M., Shiura, H., Kohda, T., Nakamuta, N., and Ogura, A. (2019). Paternal knockout of Slc38a4/SNAT4 causes placental hypoplasia associated with intrauterine growth restriction in mice. Proc. Natl. Acad. Sci. U S A *116*, 21047–21053.

Matoba, S., Wang, H., Jiang, L., Lu, F., Iwabuchi, K.A., Wu, X., Inoue, K., Yang, L., Press, W., Lee, J.T., et al. (2018). Loss of H3K27me3 imprinting in somatic cell nuclear transfer embryos disrupts post-implantation development. Cell Stem Cell *23*, 343–354.e5.

Matoba, S., and Zhang, Y. (2018). Somatic cell nuclear transfer reprogramming: mechanisms and applications. Cell Stem Cell *23*, 471–485.

Miri, K., Latham, K., Panning, B., Zhong, Z., Andersen, A., and Varmuza, S. (2013). The imprinted polycomb group gene Sfmbt2 is required for trophoblast maintenance and placenta development. Development *140*, 4480–4489.

Parmigiani, A., Nourbakhsh, A., Ding, B., Wang, W., Kim, Y.C., Akopiants, K., Guan, K.L., Karin, M., and Budanov, A.V. (2014). Sestrins inhibit mTORC1 kinase activation through the GATOR complex. Cell Rep *9*, 1281–1291.

Petit, C.S., Roczniak-Ferguson, A., and Ferguson, S.M. (2013). Recruitment of folliculin to lysosomes supports the amino acid-dependent activation of Rag GTPases. J Cell Biol *202*, 1107–1122.

Rebsamen, M., Pochini, L., Stasyk, T., de Araujo, M.E., Galluccio, M., Kandasamy, R.K., Snijder, B., Fauster, A., Rudashevskaya, E.L., Bruckner, M., et al. (2015). SLC38A9 is a component of the lysosomal amino acid sensing machinery that controls mTORC1. Nature *519*, 477–481.

Rueden, C.T., Schindelin, J., Hiner, M.C., DeZonia, B.E., Walter, A.E., Arena, E.T., and Eliceiri, K.W. (2017). ImageJ2: ImageJ for the next generation of scientific image data. BMC Bioinformatics *18*, 529.

Sachs, M., Brohmann, H., Zechner, D., Muller, T., Hulsken, J., Walther, I., Schaeper, U., Birchmeier, C., and Birchmeier, W. (2000). Essential role of Gab1 for signaling by the c-Met receptor in vivo. J. Cell Biol. *150*, 1375–1384.

Sancak, Y., Peterson, T.R., Shaul, Y.D., Lindquist, R.A., Thoreen, C.C., Bar-Peled, L., and Sabatini, D.M. (2008). The Rag GTPases bind raptor and mediate amino acid signaling to mTORC1. Science *320*, 1496–1501.

Shimobayashi, M., and Hall, M.N. (2016). Multiple amino acid sensing inputs to mTORC1. Cell Res. *26*, 7–20.

Smith, L.C., Bordignon, V., Babkine, M., Fecteau, G., and Keefer, C. (2000). Benefits and problems with cloning animals. Can. Vet. J. *41*, 919–924.

Tanaka, S., Oda, M., Toyoshima, Y., Wakayama, T., Tanaka, M., Yoshida, N., Hattori, N., Ohgane, J., Yanagimachi, R., and Shiota, K. (2001). Placentomegaly in cloned mouse concepti caused by expansion of the spongiotrophoblast layer. Biol. Reprod. *65*, 1813–1821.

Thomas, J.D., Zhang, Y.J., Wei, Y.H., Cho, J.H., Morris, L.E., Wang, H.Y., and Zheng, X.F. (2014). Rab1A is an mTORC1 activator and a colorectal oncogene. Cancer Cell *26*, 754–769.

Trapnell, C., Roberts, A., Goff, L., Pertea, G., Kim, D., Kelley, D.R., Pimentel, H., Salzberg, S.L., Rinn, J.L., and Pachter, L. (2012). Differential gene and transcript expression analysis of RNA-seq experiments with TopHat and Cufflinks. Nat. Protoc. *7*, 562–578.

Tsun, Z.Y., Bar-Peled, L., Chantranupong, L., Zoncu, R., Wang, T., Kim, C., Spooner, E., and Sabatini, D.M. (2013). The folliculin tumor suppressor is a GAP for the RagC/D GTPases that signal amino acid levels to mTORC1. Mol Cell *52*, 495–505.

Wang, L.Y., Li, Z.K., Wang, L.B., Liu, C., Sun, X.H., Feng, G.H., Wang, J.Q., Li, Y.F., Qiao, L.Y., Nie, H., et al. (2020). Overcoming intrinsic H3K27me3 imprinting barriers improves post-implantation development after somatic cell nuclear transfer. Cell Stem Cell *27*, 315–325.e5.

Wengrod, J.C., and Gardner, L.B. (2015). Cellular adaptation to nutrient deprivation: crosstalk between the mTORC1 and eIF2alpha signaling pathways and implications for autophagy. Cell Cycle *14*, 2571–2577.

Wolfson, R.L., Chantranupong, L., Saxton, R.A., Shen, K., Scaria, S.M., Cantor, J.R., and Sabatini, D.M. (2016). Sestrin2 is a leucine sensor for the mTORC1 pathway. Science *351*, 43–48.

Woods, L., Perez-Garcia, V., and Hemberger, M. (2018). Regulation of placental development and its impact on fetal growth-new insights from mouse models. Front. Endocrinol. *9*, 570.

STAR★METHODS

KEY RESOURCES TABLE

REAGENT or RESOURCE	SOURCE	IDENTIFIER
Antibodies		
Anti-(p)-4EBP1 (S65)	Cell Signaling	Cat#9451; RRID: AB_10830895
Anti-4EBP1	Cell Signaling	Cat#9452; RRID:AB_331692
Anti-SLC38A4	Santa Cruz	Cat#sc-376664; RRID: AB_11150659
Anti-GAPDH	Cell Signaling	Cat#97166; RRID: AB_2756824
Chemicals, peptides, and recombinant proteins		
Hepes-CZB medium	(Kishigami et al., 2006)	N/A
EmbryoMax KSOM Mouse Embryo Media (KSOM medium)	Sigma-Aldrich	Cat#MR-106-D
Pregnant Mare Serum Gonadotropin (PMSG)	BioVendor	Cat# RP1782721000
Human Chorionic Gonadotropin (HCG)	Sigma-Aldrich	Cat#C1063
HTF medium	Sigma-Aldrich	Cat#MR-070-D
Hyaluronidase from Bovine Testes	Sigma-Aldrich	Cat#C6762
Cytochalasin B (CB)	Sigma-Aldrich	Cat#C6762
CZB medium	(Kishigami et al., 2006)	N/A
Trichostatin A (TSA)	Sigma-Aldrich	Cat#T8552
Paraformaldehyde, 4% in PBS	ThermoFisher Scientific	Cat#J61899-AK
TRIzol™ Reagent	ThermoFisher Scientific	Cat#15596026
DNase I, RNase-free	ThermoFisher Scientific	Cat#EN0521
NEBNext Magnesium RNA Fragmentation Module	New England Biolabs	Cat#E6150S
Second Strand Buffer	ThermoFisher Scientific	Cat#10812014
Magnesium Chloride ($MgCl_2$)	Sigma-Aldrich	Cat#M1028
Dithiothreitol (DTT)	ThermoFisher Scientific	Cat#20290
dNTP Mix	ThermoFisher Scientific	Cat#18427088
dUTP Solution	ThermoFisher Scientific	Cat#R0133
RNase H	ThermoFisher Scientific	Cat#EN0201
E. coli DNA Ligase	New England Biolabs	Cat#M0205S
DNA Polymerase I	New England Biolabs	Cat#M0209S
EDTA	Santa Cruz	Cat#sc-203932
Critical commercial assays		
Dynabeads™ mRNA Purification Kit	ThermoFisher Scientific	Cat#61006
SuperScript™ III Reverse Transcriptase Kit	ThermoFisher Scientific	Cat#18080051
NEBNext Ultra™ II DNA library Prep Kit for Illumina	New England Biolabs	Cat#7103S
Deposited data		
All the sequencing data generated in this study	NCBI's Gene Expression Omnibus	GEO: GSE174174
Original western blot and microscopy images	Mendeley	Mendeley Data: https://doi.org/10.17632/jc86xfskzh.1
Experimental models: Organisms/strains		
Slc38a4 maternal knockout mice	This study	N/A
Oligonucleotides		
Guide RNA 1 for *Slc38a4* deletion: Ctgttttgtcactgagacct	This study	N/A
Guide RNA 2 for *Slc38a4* deletion: Cagtcacagcaaaagaggca	This study	N/A
Outter primer for genotyping of *Slc38a4* deletion (F): aaggaggtatggctgcagatta	This study	N/A

(*Continued on next page*)

Continued

REAGENT or RESOURCE	SOURCE	IDENTIFIER
Outter primer for genotyping of *Slc38a4* deletion (R): Ccttgtgctgtactctactctct	This study	N/A
Inner primer for genotyping of *Slc38a4* deletion (F): aaggaggtatggctgcagatta	This study	N/A
Inner primer for genotyping of *Slc38a4* deletion (R): Cgtcaccctgatcttaaatgca	This study	N/A
Software and algorithms		
Trim Galore	Felix Krueger in Babraham Institute	https://doi.org/10.5281/zenodo.5127899
TopHat (v2.1.1)	(Kim et al., 2013)	http://github.com/infphilo/tophat
Cufflinks (v2.2.1)	(Trapnell et al., 2012)	http://cole-trapnell-lab.github.io/cufflinks/getting_started/
Ingenuity Pathway Analysis (IPA)	Qiagen	N/A
ImageJ	(Rueden et al., 2017)	https://imagej.nih.gov/ij/download.html
DAVID	(Huang da et al., 2009)	https://david.ncifcrf.gov/

RESOURCE AVAILABILITY

Lead contact

Further information and request for reagents and resources should be directed to and will be fulfilled by the lead contact, Yi Zhang (yzhang@genetics.med.harvard.edu)

Materials availability

All unique/stable reagents generated in this study is available from the lead contact with a completed Materials Transfer Agreement.

Data and code availability

All the sequencing data generated in this study have been deposited at GEO and are publicly available as of the date of publication. Accession numbers are listed in the key resources table. Original western blot and microscopy images have been deposited at Mendeley and are publicly available as of the data of publication. The DOI is listed in the key resources table.

This paper does not report original code.

EXPERIMENTAL MODEL AND SUBJECT DETAILS

8–10 weeks old healthy female mice of C57BL/6J or B6D2F1 (C57BL/6J × DBA/2J) strain were selected to use in this study. Mice were housed with nesting material, free access to food and water, controlled temperature and a 12:12 h light-dark cycle. Mice were not involved in previous procedures and were drug and test naïve. The mouse maintenance and experiments were performed following the approved protocols by the Institution Animal Care and Use Committee (IACUC) of Harvard Medical School.

METHOD DETAILS

Generation of *Slc38a4* maternal knockout (MKO) female mice for SCNT

To generate *Slc38a4* MKO female mice, a pair of guide RNAs targeting exon 3 of *Slc38a4* were firstly designed. The guide RNA pairs (50 ng/μL) and *Cas9* mRNA (100 ng/μL) were injected into one blastomere of 2-cell embryo (C57BL/6J) using a piezo-driven system in Hepes-CZB medium. After injection, the 2-cell embryos were cultured in KSOM medium with amino acids transiently and then transferred to the pseudo-pregnant mother. The new-born mice were then genotyped to select for the *Slc38a4* mutant female founder mice. The *Slc38a4* mutant female founder mice were bred with wild type (WT) male (C57BL/6J) mice to generate the *Slc38a4* MKO female mice (C57BL/6J). Then, the *Slc38a4* MKO female mice (C57BL/6J) were further crossed with WT male mice (DBA/2J) to generate the *Slc38a4* MKO female mice in B6D2F1 background. The cumulus cells from *Slc38a4* MKO female mice in B6D2F1 background at the age of 8–10 weeks were collected for SCNT experiments. The cumulus cells from wild-type female mice in the same B6D2F1 background were collected for control SCNT experiments.

In vitro fertilization (IVF)

Female mice (C57BL/6J) of 8–10 weeks were used to induce superovulation by injection of 5 IU of Pregnant Mare Serum Gonadotropin (PMSG) and 5 IU of Human Chorionic Gonadotropin (HCG) at an interval of 48 h. Sperms were collected from the epididymis of

male mice (DBA/2J) and preactivated in HTF medium for 1 h at 37°C in humidified atmosphere with 5% CO_2. The B6 cumulus-oocyte complexes (COCs) were collected 14–15 h after HCG injection in HTF medium and *in vitro* fertilized with preactivated sperm. After incubation for 2–3 hours, the COCs were dissociated and the zygotes were washed and cultured in HTF medium for another 4–6 hours. Zygotes with 2-pronuclei were picked and transferred to KSOM medium with amino acids before embryo transfer at 2-cell stage.

Somatic cell nuclear transfer (SCNT)

The somatic cell (cumulus cell) nuclear transfer was performed as previously described (Kishigami et al., 2006) with minor modification. Briefly, MII oocyte were first collected from 8–10 weeks of WT female mice (B6D2F1) at 14h after superovulation. The cumulus-oocyte complexes were dissociated in Hepes-CZB medium supplied with Hyaluronidase from Bovine Testes. The cumulus cells were then collected from 8–10 weeks of WT or *Slc38a4* MKO female mice (B6D2F1) as nuclear donors. The oocyte was enucleated in Hepes-CZB medium containing 5 μg/mL cytochalasin B (CB) by blunt piezo-driven pipette. The enucleated oocytes were washed and cultured in CZB medium for 1h, and then the donor nucleus of cumulus cell was injected into the enucleated oocyte directly. After culturing in CZB medium for 1h, the reconstructed embryos were activated in Ca^{2+} free CZB medium containing 5 mM Sr^{2+}, 50 ng/mL Trichostatin A (TSA) and 5 μg/mL CB for 5 hours, and then transferred to KSOM medium supplemented with 50 ng/mL TSA for another 2.5 ∼ 3.5 h. Eventually, the reconstructed embryos were thoroughly washed and cultured in KSOM medium with amino acids at 37°C in humidified atmosphere with 5% CO_2 before embryo transfer at 2-cell stage.

Embryo transfer and cesarian section

2-cell embryos were transferred into the oviduct of 0.5 days post coitus (dpc) pseudo-pregnant mother. Cesarian section was performed at E9.5, E14.5 and E19.5 respectively.

Hematoxylin and eosin (HE) staining

The placentae collected at E14.5 and E19.5 were fixed with 4% paraformaldehyde overnight. The fixed placentas were sent to the Rodent Histopathology Core (220 Longwood Ave., Boston, MA, USA) for paraffin embedding, section and HE staining.

Transcriptome profiling

Spongiotrophoblast from placentae was dissected and lysed with TRIzol reagent. RNA was extracted by isopropanol precipitation. 10 μg RNA was DNase I treated at 37°C for 1 hour. RNA with poly-A tail was then captured and purified using Dynabeads™ mRNA Purification Kit according to the manufacturer's instructions. Purified RNA was fragmented with RNA Fragmentation Module at 95°C for 5 min. Reaction was then stopped and RNA was purified. First stand cDNA was synthesized using SuperScript™ III Reverse Transcriptase Kit according to the manufacturer's instructions. Second strand cDNA was synthesized with Second Strand Buffer, $MgCl_2$, DTT, dNTP, dUTP, RNase H, *E. coli* DNA Ligase and DNA Polymerase I. DNA was purified after 2-hour incubation on thermomixer at 16°C. Synthesized cDNA was subjected to library preparation using NEBNext Ultra™ II DNA library Prep Kit for Illumina according to manufacturer's instructions.

Metabolome profiling

40–50 μL blood was collected from individual E19.5 euthanized embryo. The blood was mixed with 5 μL 0.5M EDTA and incubated at 4°C for 5 minutes. After centrifugation at 1,200 × g for 10 min at 4°C, 10–15 μL plasma obtained from each embryo was mixed with 4-folds volume of cold methanol. After incubation at −80°C for 6–8 hours, the mixture was centrifuged at 14,000 × g at 4°C for 10 minutes, and the supernatant was transferred to a new microcentrifuge tube. The supernatant was concentrated without heat and sent for CE-TOFMS analysis.

QUANTIFICATION AND STATISTICAL ANALYSIS

Processing of RNA sequencing data

Adaptors of all sequenced reads were firstly trimmed by Trim Galore with parameters –illumina –paired. Purified reads were then mapped to the mm9 reference genome using TopHat with parameters -p 2 -g 1 –no-coverage-search. Then, expression values represented by fragments per kilobase per million (FPKM) of the protein-coding genes were calculated by Cufflinks based on annotations from Ensembl database.

Identification of rescued genes in MKO SCNT placentae

Firstly, the average FPKM of each gene in two replicates of IVF, WT SCNT and MKO SCNT placentae was calculated. Genes with average FPKM $\geq$1 in IVF or WT SCNT placentae were considered as expressed and the expressed genes with a 1.5-fold change in FPKM were considered as upregulated or downregulated genes in WT SCNT placentae. Then, in those dysregulated genes, the ones showed average FPKM $\geq$ 1 in WT SCNT or MKO SCNT placentae and a 1.5-fold change in FPKM in MKO SCNT placentae (rescued from WT SCNT placentae) were annotated as the rescued genes in MKO SCNT Placentae.

The rescued genes in MKO SCNT placentae were sent for pathway analysis by QIAGEN Ingenuity Pathway Analysis (QIAGEN IPA) and gene functional assay by DAVID.

Analysis of allelic gene expression

Transcriptomes of IVF and SCNT mouse placentae (C57BL/6J × PWK/PhJ) at E10.5 were collected from a public dataset (Wang et al., 2020), and aligned to mouse genome as described above. Then, single-nucleotide polymorphisms (SNPs) derived from C57BL/6J and PWK/PhJ stains located within the exons of *Slc38a4* were identified out according to the previous study (Danecek et al., 2011). Based on those SNPs, the aligned reads were assigned to paternal or maternal alleles. Finally, the total reads assigned to each allele were used to represent the allelic expression levels of *Slc38a4.*

Quantification of western blot

The quantification of p-4EBP1 and 4EBP1 from Western blot was performed by ImageJ. To calculate the relative intensity of p-4EBP1/4EBP1 integrating different samples from different membranes, average signal of p-4EBP1 or 4EBP1 on each membrane was first quantified. Then, on each membrane, the relative signal of p-4EBP1 or 4EBP1 in individual sample was calculated by dividing individual signal of p-4EBP1 or 4EBP1 with the average signal on that membrane. The final relative intensity of p-4EBP1/4EBP1 for each sample was calculated by dividing the relative signal of p-4EBP1 with the relative signal of 4EBP1 of that sample.